

Set-Based Threat Assessment in Semi-Autonomous Vehicles

Paolo Falcone* Mohammad Ali*,** Jonas Sjöberg*

* Chalmers University of Technology, Dept. of Signals and Systems,
412 96 Göteborg (e-mail: falcone@chalmers.se,
jonas.sjoberg@chalmers.se).

** Volvo Car Corporation, Dept. of Vehicle Dynamics & Active Safety,
96250/PV4A, 405 31 Göteborg (e-mail: mali21@volvocars.com).

Abstract: We present a model based threat assessment method for semi-autonomous vehicles. Based on the assumption that information about the surrounding environment is available over a future finite time horizon, we first introduce a set of constraints on the vehicle states, which are satisfied under “safe” driving conditions. Then, we use vehicle and driver mathematical models in order to predict future constraints violation, indicating the possibility of accident or loss of vehicle control.

We demonstrate the proposed method in a roadway departure application, and validate it through experimental data.

Keywords: Threat Assessment, Active Safety, Semi-Autonomous Vehicles, Invariant Sets Theory.

1. INTRODUCTION

In vehicles equipped with classical active safety systems like, e.g. yaw stability control, the vehicle motion within the environment is primarily determined by the driver, whereas the active safety systems merely affect the dynamical behavior of the vehicle.

Advanced Driver Assistance Systems (ADAS), instead, can implement complex accident prevention functions by influencing both the vehicle dynamical behavior and its motion within the surrounding environment. Such advanced active safety functions have been primarily enabled by recent advances in sensing technologies, which led to affordable onboard sensors providing the vehicle position and velocity in a global frame as well as information about the surrounding environment like, e.g., road geometry and relative position and velocity of moving objects. The current trend in the development of ADAS points in the direction of increased authority in controlling the vehicle motion in the environment Mellinger et al. (2009). Example of such trend are, e.g., the lane guidance systems assisting the driver in maintaining the vehicle within the lane boundaries.

Early lane guidance systems, based on lateral vehicle control, were presented already in Pomerleau (1995). Lateral control for lane guidance and highway automation applications has then been recently further investigated in, among others, Hiraoka et al. (2009); Minoiu E. et al. (2009); Shin et al. (2008); Netto et al. (2004). In Hiraoka et al. (2009) a path tracking controller based on sliding mode control is proposed and demonstrated. In Minoiu E. et al. (2009) the lateral controller is instead derived using LMI and Lyapunov theory. In Shin et al. (2008), the authors implement a lateral controller using backstepping

techniques while in Netto et al. (2004) the lateral control problem is solved by an adaptive controller. Most of the mentioned lane guidance approaches can be classified as autonomous driving systems, since they do not account for the presence of the driver. In active safety applications, instead, an intervention (or warning) should be issued if and only if a risk of lane departure (or, in general, accident) is detected, that the driver is not able to avoid. Hence, active safety problems involve challenges which do not occur in completely autonomous driving problems. In particular, in an active safety problem, an autonomous driving intervention might be experienced as intrusive by the driver. It is thus essential that autonomous driving is initiated if and only if it is needed. The formulation of transition conditions, between the different modes of a safety system, is not trivial.

The “*Time to Line Crossing*” (TLC) is used in several lane guidance algorithms to represent the threat level and it is among the most common approaches used to formulate a transition condition. In particular, an intervention or warning is issued once TLC passes a predefined threshold. An excellent overview and assessment of methods for calculating the TLC is provided in Mammar et al. (2006).

An approach, based on artificial potential fields, is presented in Rossetter and Gerdes (2002). This approach is derived from robotic control and is attractive since it allows several different driver assistance systems to be implemented using the same framework. The potential fields are defined such that lane crossings are prevented in the absence of driver inputs with focus on guaranteeing that the system tends towards a safer state. An optimization based approach, for a semi-autonomous vehicle, is presented in Anderson et al. (2009) where an assisting intervention is

issued once a trajectory, computed by a Model Predictive Controller, is considered hazardous.

However, we believe that a weakness of these approaches is that *the transition thresholds activating the autonomous interventions are based on limitations of a controller rather than limitations in the driver's ability to stay in the lane*. This might lead to initiation of the autonomous intervention, in order to guarantee safe operation of the controller, in situations where the driver does not need assistance. Alternatively, if the controller is outperforming, no intervention might be issued at all.

In this paper, we present a model based method for evaluating the driver's ability in safely performing a desired maneuver. We first introduce a set of constraints describing a "safe" driving. Moreover, we assume the road geometry is available over a future finite time horizon and exploit the vehicle and driver modeling in order to predict future constraints violation, indicating the possibility of accident or loss of vehicle control. We demonstrate the proposed method in a roadway departure application, and validate it through experimental data. The paper is organized as follows. In Section 2, we provide basic definitions and results on set invariance theory. In Section 3, we present the vehicle and driver modeling used next in Section 4, where the threat assessment algorithm is presented. In Section 5, we validate the proposed algorithm through experimental data, while Section 6 closes the paper with final remarks.

2. BACKGROUND ON SET INVARIANCE THEORY

In this section we introduce few definitions and recall basic results on set invariance theory. We will denote the set of all real numbers and positive integers by \mathbb{R} and \mathbb{N}^+ , respectively.

Definition 1. A polyhedron is a set that equals the intersection of a finite number of closed half spaces.

2.1 Background on Invariant Sets

This section adopts the notation used in Grieder (2004) and provides the basic definitions for invariant sets for constrained systems. A comprehensive survey of papers on set invariance theory can be found in Blanchini (1999).

Denote by f_a the state update function of an autonomous system

$$x(t+1) = f_a(x(t), w(t)), \quad (1)$$

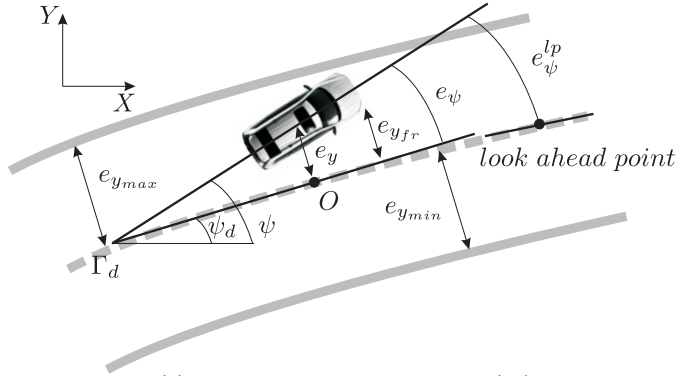
where $x(t)$ and $w(t)$ denote the state and disturbance vectors, respectively. System (1) is subject to the constraints

$$x(t) \in \mathcal{X} \subseteq \mathbb{R}^n, \quad w(t) \in \mathcal{W} \subseteq \mathbb{R}^d, \quad (2)$$

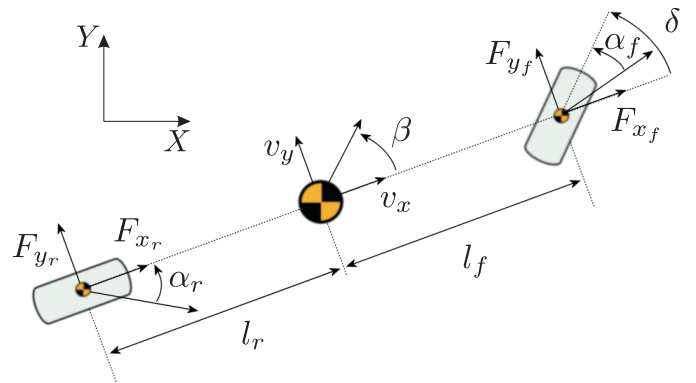
where \mathcal{X} and \mathcal{W} are polyedra containing the origin in their interior.

For the autonomous system (1)-(2), we will denote the set of states that evolves to \mathcal{S} in one step as

$$\text{Pre}_{f_a}(\mathcal{S}, \mathcal{W}) \triangleq \{x \in \mathcal{X} \mid f_a(x, w) \in \mathcal{S}, \forall w \in \mathcal{W}\}. \quad (3)$$



(a) Definition of control errors in (13)



(b) Notation for the single track model.

Fig. 1. Vehicle modeling.

Similarly, for the nominal system, i.e., $w = 0$,

$$\text{Pre}_{f_a}(\mathcal{S}) \triangleq \{x \in \mathcal{X} \mid f_a(x, 0) \in \mathcal{S}\}. \quad (4)$$

The following definitions are derived from Blanchini (1999); Kolmanovsky and Gilbert (1998).

Definition 2. (Robust positive Invariant Set). A set \mathcal{O} is said to be a robust positive invariant set for the autonomous system (1) subject to the constraints in (2), if

$$x(0) \in \mathcal{O} \Rightarrow x(t) \in \mathcal{O}, \quad \forall t \in \mathbb{N}^+.$$

Definition 3. (Maximal Robust Positive Invariant Set \mathcal{O}_∞).

The set \mathcal{O}_∞ is the maximal robust invariant set of the autonomous system (1) subject to the constraints in (2), if $0 \in \mathcal{O}_\infty$, \mathcal{O}_∞ is a robust positive invariant set and \mathcal{O}_∞ contains all the robust positive invariant sets contained in \mathcal{X} that contain the origin.

3. MODELING

In this section, we present the vehicle and driver mathematical models used in Section 4, as basis of the threat assessment algorithm.

3.1 Vehicle Modeling

Consider the vehicle model sketched in Figure 1. The vehicle motion within the lane, subject to the lateral and yaw dynamics, is described by the following set of differential equations

$$m\dot{v}_y = -mv_x\dot{\psi} + 2[F_{y_f} + F_{y_r}], \quad (5a)$$

$$J_z\dot{\psi} = 2[l_f F_{y_f} - l_r F_{y_r}], \quad (5b)$$

$$\dot{e}_\psi = \dot{\psi} - \dot{\psi}_d, \quad (5c)$$

$$\dot{e}_y = v_y + v_x e_\psi, \quad (5d)$$

where m and J_z denote the vehicle mass and yaw inertia, respectively, l_f and l_r are the distances of the vehicle center of gravity from the front and rear axles, respectively, v_x and v_y are the longitudinal and lateral velocities, respectively, in the vehicle body frame, $\dot{\psi}$ is the turning rate, where ψ denotes the vehicle orientation w.r.t. the fixed global frame (X, Y) in Figure 1(a). F_{yf} , F_{yr} are the lateral tire forces at the front and rear axles, respectively. In (5c) and (5d), e_ψ and e_y denote the vehicle orientation and position errors, respectively, w.r.t. the road centerline and ψ_d is the desired vehicle orientation, i.e., the slope of the tangent to the curve Γ_d in the point O .

The lateral tire forces in (5a) and (5b) are generated at the tire contact patch and are, in general, nonlinear functions of the vehicle states. Accurate physical modeling of tire forces is quite involving and several models have been proposed in the literature over the past two decades. An exhaustive review of existing tire models can be found in Svdenius (2007). In this paper, we compute the lateral tire forces as

$$F_{y,i} = -C_i \alpha_i, \quad i \in \{f, r\}, \quad (6)$$

where C_i are the tire cornering stiffness coefficients at the two axles and α_i are the tire slip angles which, for small values, can be approximated as

$$\alpha_f = \frac{v_y + l_f \dot{\psi}}{v_x} - \delta, \quad (7a)$$

$$\alpha_r = \frac{v_y - l_r \dot{\psi}}{v_x}, \quad (7b)$$

with δ denoting the front steering angle.

Remark 1. The simplified linear tire model (6) well approximates more complex nonlinear tire characteristics Bakker et al. (1989) for small tire slip angles, i.e., $\alpha_i \in [\alpha_{i,min}^*, \alpha_{i,max}^*]$. However, this interval also corresponds to a “normal driving” region where drivers usually operate Rajamani (2006); Kiencke and Nielsen (2005).

In order to avoid possible vehicle instability due to the effects of the tire nonlinearities (see Remark 1), the vehicle is forced to operate in a region of the state space corresponding to limited values of the vehicle body side slip angle β

$$\beta_{min} \leq \beta \leq \beta_{max}, \quad (8)$$

where β can be approximated as $\beta = \frac{v_y}{v_x}$.

Furthermore, constraints on vehicle position are set by the limited lane width. In order to formulate the constraints on the vehicle position within the lane, we denote by $e_{y_{ij}}$, $i \in \{f, r\}$, $j \in \{l, r\}$ the distances of the four vehicle corners from the lane centerline. By assuming small orientation errors,

$$\begin{aligned} e_{y_{fl}} &= e_y + \frac{c}{2} + a e_\psi, & e_{y_{fr}} &= e_y - \frac{c}{2} + a e_\psi, \\ e_{y_{rl}} &= e_y + \frac{c}{2} - b e_\psi, & e_{y_{rr}} &= e_y - \frac{c}{2} - b e_\psi, \end{aligned} \quad (9)$$

where c is the vehicle width, a and b are the distances of the center of gravity from the front and rear vehicle bumpers, respectively.

The constraints on the vehicle position are written as

$$e_{y_{min}} \leq e_{y_{ij}} \leq e_{y_{max}}, \quad i \in \{f, r\}, \quad j \in \{l, r\}, \quad (10)$$

where $e_{y_{min}}$ and $e_{y_{max}}$ set the maximum allowed deviation from the lane centerline.

The model (5)-(9), along with the constraints (8), (10), can be compactly written as

$$\dot{x}(t) = Ax(t) + Bu(t) + Ew(t) \quad (11a)$$

subj. to

$$Hx(t) \leq K, \quad (11b)$$

where $x = [v_y, \dot{\psi}, e_\psi, e_y]$, $u = \delta$ and $w = \dot{\psi}_d$ are the state, the input and the disturbance vectors, respectively.

3.2 Driver Modeling

In this section, we start from the vehicle model (5) and present a feedback control law resembling the human driver's steering behavior while performing a lane following task. This, combined with the vehicle model (11), is used next as basis of the threat assessment algorithm.

The literature on the modeling of driver steering is enormous. Early studies on driver modeling date back to the sixties and demonstrated the importance of preview information for human drivers Roland and Sheridan (1967). McRuer *et al.* were among the first proposing a human driver's steering algorithm consisting of an open loop “pursuing” part and a closed loop correcting part McRuer et al. (1977). The results in McRuer et al. (1977) led to the conclusion that the pursuit part, based on the preview of the desired path, generates most of the driver's steering command. This conclusion is the basis of the “preview control” algorithms, extensively studied in the seventies. The various preview control algorithms can be divided in two main groups, depending on whether the “preview signal” is provided as a (i) reference or (ii) a disturbance Peng and Tomizuka (1993). In the driver model used in this manuscript, the “preview signal” enters as a disturbance and the controller has a feedback/feedforward structure.

Define the orientation error e_ψ^{lp} , w.r.t. the look-ahead point in Figure 1(a), as

$$\begin{aligned} e_\psi^{lp} &= \psi - \psi_d^{lp} \\ &= e_\psi + \Delta\psi_d, \end{aligned} \quad (12)$$

where ψ_d^{lp} is the desired orientation at time $t + t_{lp}$, with t the current time, t_{lp} the preview time and $\Delta\psi_d = \psi_d - \psi_d^{lp}$.

Remark 2. The preview signal ψ_d^{lp} is defined w.r.t. to the preview time t_{lp} . This can be mapped into the preview distance d_{lp} traveled by the vehicle along the curve Γ_d from the point O , at constant speed v_x .

We consider the vehicle model (5) and compute the steering angle δ as

$$\begin{aligned} \delta &= -K_y e_y - K_\psi e_\psi^{lp}, \\ &= -K_y e_y - K_\psi e_\psi - K_\psi \Delta\psi_d, \end{aligned} \quad (13)$$

with K_y , K_ψ gains that are, in general, time varying and might be online updated. In this paper, the gains K_y , K_ψ

are constant and off-line estimated by using a least squares method and experimental data. In Section 5, we show validation results of the model (13).

Remark 3. We observe that the driver's steering command computed in (13) consists of a linear state feedback term and a feedforward term depending on the desired orientation at the look-ahead point, i.e., the preview information.

Remark 4. Clearly, $\Delta\psi_d$ in (12) depends on the preview time t_{lp} that, in our modeling framework, is considered as a parameter of the driver's model. Hence, as K_y and K_ψ , t_{lp} can be identified from experimental data.

3.3 Closed Loop System

We consider the constrained autonomous system, obtained by combining the vehicle model (5), along with the constraints (8), (10), with the driver model (13), that can be compactly written as

$$\dot{x}_{cl}(t) = A_{cl}x_{cl}(t) + E_{cl}w_{cl}(t) \quad (14a)$$

subj. to

$$H_{cl}x_{cl}(t) \leq K_{cl}, \quad (14b)$$

where $x_{cl} = [v_y, \dot{\psi}, e_\psi, e_y]$ and $w_{cl} = [\dot{\psi}_d, \Delta\psi_d]$ are the state and the disturbance vectors, respectively. The matrices A_{cl} , E_{cl} , H_{cl} and K_{cl} are omitted due to lack of space.

We observe that both $\dot{\psi}_d$ and $\Delta\psi_d$ in w_{cl} describe the road geometry.

4. SET BASED THREAT ASSESSMENT

4.1 Main Algorithm

We discretize the model (14) with a sampling time T_s , to obtain the discrete time constrained autonomous system with disturbances

$$x_{cl}(t+1) = A_{cl}^d x_{cl}(t) + E_{cl}^d w_{cl}(t) \quad (15a)$$

subj. to

$$H_{cl}x_{cl}(t) \leq K_{cl}, \quad (15b)$$

where, for the sake of simple notation, we have denoted the state, the disturbance and the time index with the same symbols as in (14).

We introduce the following assumptions on the disturbance signal w_{cl}

Assumption 1. $w_{cl}(t) \in \mathcal{W}$, $\forall t \geq 0$, where $\mathcal{W} \subseteq \mathbb{R}^2$ is a polyhedron that contains the origin in its interior.

Assumption 2. Every time instant t , the disturbance $w_{cl}(t)$ is known over a finite time horizon of N steps.

Remark 5. We recall that, every time instant t , the second component of the disturbance vector, i.e. $\Delta\psi_d$, is based on the desired orientation ψ_d^{lp} at time $t + N_{lp}$ with $N_{lp} = t_{lp}/T_s$ (see (12)). This is the desired vehicle orientation at the look-ahead point, see Remark 2. Hence, the Assumption 2 on the disturbance w_{cl} requires the knowledge of the road geometry over a future time horizon of N_{lp} steps.

We denote by \mathcal{X}_{feas} the set of admissible states

$$\mathcal{X}_{feas} = \{x \in \mathbb{R}^4 : H_{cl}x \leq K_{cl}\}. \quad (16)$$

Every time instant, we consider a terminal target set $\mathcal{T} \subseteq \mathcal{X}_{feas}$. Further details about the choice of \mathcal{T} are provided next in Section 4.2.

Denote by $W_t = [w_t, w_{t+1}, \dots, w_{t+N-1}]$, the sequence of disturbance samples over the time horizon $[t, t+N-1]$ and by $W_{t,i} = [w_{t+i}, \dots, w_{t+N-1}]$ any sequence extracted from W_t . We compute the sequence of states sets $X_t(W_t) = [\mathcal{X}_t, \mathcal{X}_{t+1}, \dots, \mathcal{X}_{t+N-1}]$ as:

$$\mathcal{X}_{t+i}(W_{t,i}) = \mathcal{X}_{feas} \bigcap \text{Pre}_{f_a}(\mathcal{X}_{t+i+1}, w_{t+i}), \quad (17a)$$

$$i = N-1, \dots, 0,$$

$$\mathcal{X}_{t+N} = \mathcal{T}, \quad (17b)$$

where, f_a denotes the right hand side of the (15a). We call the set \mathcal{X}_t the *safe set* at time t .

We observe that the calculation of the sequence $X_t(W_t)$ is performed every time step, based on the updated disturbance sequence W_t . Moreover, if at the current time t the state of the system (15) belongs to the safe set \mathcal{X}_t , the autonomous system (15), i.e., the vehicle in closed loop with the driver, is guaranteed to evolve to the set \mathcal{T} in N steps, while satisfying the constraints (15b).

In summary, the proposed threat assessment algorithm is made of three main steps to be performed every time step

- (1) select the terminal target set \mathcal{T} ,
- (2) based on the future disturbance sequence W_t and the set \mathcal{T} , perform the backward calculation of the sequence of safe sets \mathcal{X}_{t+i} according to (17),
- (3) check whether the current state $x_{cl}(t)$ belongs to the safe set \mathcal{X}_t , in order to assess the driver's ability in safely driving the vehicle from the current state to the target set \mathcal{T} over the future horizon of N steps.

Clearly, if the state does not belong to the safe set \mathcal{X}_t , an action is required in order to "enlarge" the safe set to enclose the current state. Such an action might be the activation of a driver assistance system.

As last remark of this section, we observe that the proposed algorithm guarantees a "safe" (i.e., with guarantee of constraints satisfaction) reaching of the target set \mathcal{T} . In general, the driver is not guaranteed to keep the vehicle within \mathcal{T} after the time $t+N$. In the next section we comment the choice of the target set \mathcal{T} and propose a method for guaranteeing constraint satisfaction, i.e., that the driver will maintain the vehicle within \mathcal{T} , for $t > t+N$.

4.2 Terminal Set

The choice of the terminal set \mathcal{T} in the threat assessment algorithm proposed in Section 4.1 affects the *effectiveness* and the *conservativeness* of the algorithm. Indeed, the simplest choice is setting $\mathcal{T} = \mathcal{X}_{feas}$. In this case, the algorithm guarantees only a safe driving over the future N steps.

As alternative, the set \mathcal{T} could be chosen as $\mathcal{T} = \mathcal{O}_\infty$, where $\mathcal{O}_\infty \subseteq \mathcal{X}_{feas}$ is the maximal robust positive invariant set for the autonomous system (15a) subject to the constraints (15b). We recall that in this case,

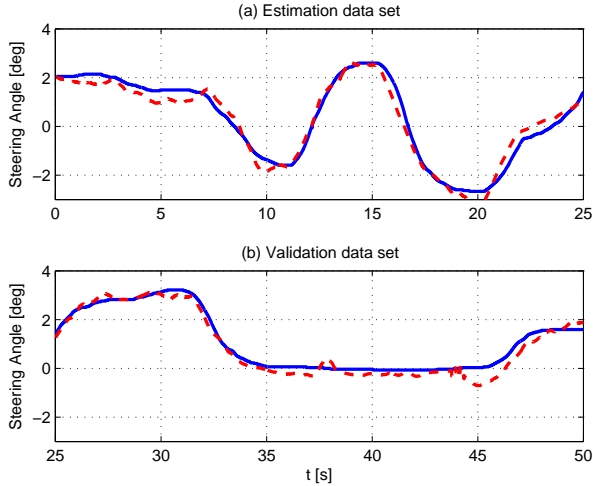


Fig. 2. Validation of the driver model. The solid lines is the measured driver's steering angle, while the dashed line is the steering predicted through model (13).

$x(t+N) \in \mathcal{O}_\infty \Rightarrow x(t+N+k) \in \mathcal{O}_\infty, \forall w(t) \in \mathcal{W}, k \in \mathbb{N}^+$, that is, the vehicle will be kept within the lane, despite all admissible lane curvature beyond the look-ahead point. Setting the final set equal to the maximal robust positive invariant set might lead to high conservativeness of the threat assessment algorithm.

5. RESULTS

The algorithm presented in Section 4 has been experimentally validated on a test track. Full state measurements have been obtained through a differential GPS, a built-in high precision gyro and a digital map. The test track resembles a country road, with several sharp curves. In order to assess the algorithm performance in a wide range of operating conditions, the vehicle has been driven several laps with both normal and slightly rougher driving style, yet without activating any stability system.

We first show the validation results of the driver model (13). The data used for parameters estimation have been collected in normal driving. The problem of estimating the parameters K_y , K_ψ and t_{lp} in (13) has been formulated as a nonlinear least squares problem since the driver model is linear only in the parameters K_y , K_ψ . The nonlinear least squares method, described in Kay (1993), has been used. The data set used for parameters identification is shown in Figure 2(a), while the validation data set is displayed in Figure 2(b). The results in Figure 2(b) show a good matching between the driver's steering, predicted by the model (13), and measurements.

The driver model (13) has been used to validate, through experimental data, the threat assessment algorithm presented in Section 4. We have considered a scenario where the driver is negotiating the curve in Figure 3(a) at a constant speed of 90 km/h. We have considered the vehicle positions 1 and 2 on the track, shown in figure 3(a). Denote by t_1 and t_2 the time instants, when the vehicle is in positions 1 and 2, respectively. The dashed lines starting from the vehicle denote the horizon of N steps, over which

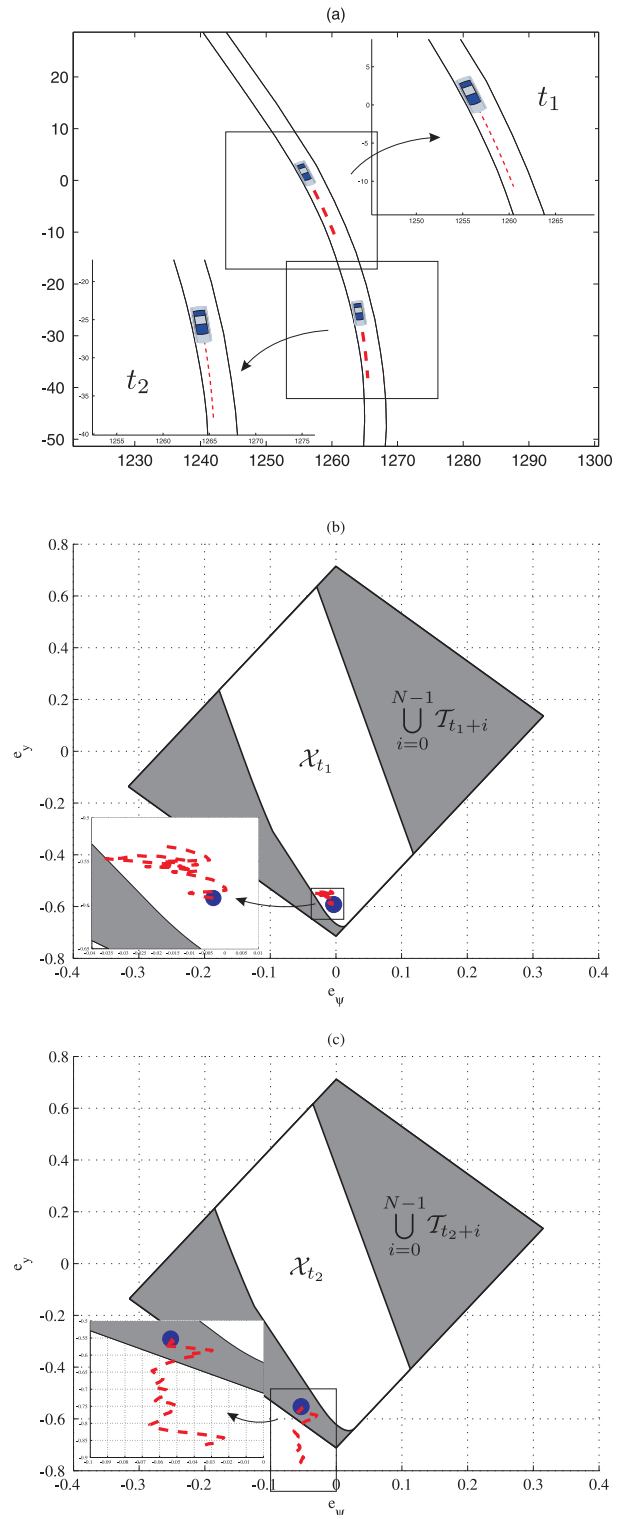


Fig. 3. Plot (a) shows the vehicle while negotiating a curve. Plot (b) shows the safe set at point 1 in (a) while plot (c) shows the safe set at point 2. In plots (b) and (c), the circles denote the current state while the dashed line shows the state trajectory over the horizon.

the disturbance is assumed to be known. In the two vehicle positions we have computed the safe sets \mathcal{X}_{t_1} and \mathcal{X}_{t_2} , respectively, according to the threat assessment algorithms in Section 4, where we have set $\mathcal{T} = \mathcal{X}_{feas}$ as terminal set and used the following parameters

$$\begin{aligned} \beta_{max} = -\beta_{min} = 7.1^\circ, \quad v_x = 90km/h, \quad t_{lp} = 0.8s, \\ N = 50, \quad T_s = 0.01s, \quad e_{y_{max}} = -e_{y_{min}} = 1.56m. \end{aligned}$$

In Figures 3(b) and 3(c) the polyedra $\mathcal{X}_{t_1}^{3,4}$ and $\mathcal{X}_{t_2}^{3,4}$, where

$$\mathcal{X}_t^{3,4} = \mathcal{X}_t \cap \left\{ x \in \mathbb{R}^4 : \begin{bmatrix} 1 & 0 & 0 & 0 \\ 0 & 1 & 0 & 0 \end{bmatrix} x = \begin{bmatrix} x_{cl}^1(t) \\ x_{cl}^2(t) \end{bmatrix} \right\} \quad (18)$$

and the superscript i in $x_{cl}^i(t)$ denote the i -th component of the vector $x_{cl}(t)$, are shown. The states $x_{cl}(t_1)$ and $x_{cl}(t_2)$ are marked with a circle in Figures 3(b) and 3(c), respectively. We observe that $x_{cl}(t_1) \in \mathcal{X}_{t_1}^{3,4}$ and $x_{cl}(t_2) \notin \mathcal{X}_{t_2}^{3,4}$. Hence, from the initial state $x_{cl}(t_1)$, the vehicle will safely travel over a horizon of N steps while, from the initial state $x_{cl}(t_2)$, the vehicle state trajectory will violate the constraints (16). This is confirmed by the measured state trajectories, reported in Figures 3(b) and 3(c) with dashed lines. In particular, in Figure 3(b), starting from the initial state $x_{cl}(t_1)$, the state trajectory entirely evolves within

the set $\mathcal{T}_1 = \bigcup_{t=t_1}^{t_1+N-1} \mathcal{T}^{3,4}$, where the sets $\mathcal{T}^{3,4}$ are obtained by replacing \mathcal{X}_t with \mathcal{T} in (18). In Figure 3(c), instead, we observe that the state trajectory leaves the set $\mathcal{T}_2 = \bigcup_{t=t_2}^{t_2+N-1} \mathcal{T}^{3,4}$, i.e., the vehicle violates the bounds on the lateral deviation from the lane centerline.

6. CONCLUSION

We have presented a model based threat assessment method for semi-autonomous driving. First a set of constraints is introduced describing a “safe” driving. Then, based on the knowledge of the road geometry over a future finite time horizon, the vehicle and driver modeling, set invariance theory is used to calculate a sequence of safe states sets. The validation of the proposed method with experimental results, demonstrates that the method effectively predicts a constraints violation, possibly indicating vehicle instability and/or lane crossing.

REFERENCES

- Anderson, S.J., Peters, S.C., Pilutti, T.E., and Iagnemma, K.D. (2009). An Optimal-Control-Based Framework for Trajectory Planning, Threat Assessment, and Semi-Autonomous Control of Passenger Vehicles in Hazard Avoidance Scenarios: Experimental Results. *In Proc. Conference on Field and Service Robots*.
- Bakker, E., Nyborg, L., and Pacejka, H. (1989). Tyre Modeling for Use in Vehicle Dynamics Studies. *SAE*, Paper 870421.
- Blanchini, F. (1999). Set invariance in control — a survey. *35(11)*, 1747–1768.
- Grieder, P. (2004). *Efficient Computation of Feedback Controllers for Constrained Systems*. Ph.D. thesis.
- Hiraoka, T., Nishihara, O., and Kumamoto, H. (2009). Automatic path-tracking controller of a four-wheel steering vehicle. *Vehicle System Dynamics*. doi: 10.1080/00423110802545919.
- Kay, S.M. (1993). *Fundamentals of statistical signal processing: estimation theory*. Prentice hall signal processing series.
- Kiencke, U. and Nielsen, L. (2005). *Automotive Control Systems*. Springer.
- Kolmanovsky, I. and Gilbert, E.G. (1998). Theory and computation of disturbance invariant sets for discrete-time linear systems. *Mathematical Problems in Engineering*, 4, 317–367.
- Mammar, S., Glaser, S., and Netto, M. (2006). Time to Line Crossing for Lane Departure Avoidance: A Theoretical Study and an Experimental Setting. *IEEE Transactions on Intelligent Transportation Systems*, 7, 226–241.
- McRuer, D.T., Allen, R.W., Weir, D.H., and Klein, R.H. (1977). New results in driver steering control models. *Human Factors*.
- Mellinghoff, U., Breitling, T., Schöneburg, R., and Metzler, H.G. (2009). The Mercedes-Benz Experimental Safety Vehicle 2009. *In Proc. International Technical Conference on the Enhanced Safety of Vehicles Conference (ESV)*, 1–11.
- Minoiu E., N., Mammar, S., Netto, M., and Lusetti, B. (2009). Driver Steering Assistance for Lane-Departure Avoidance Based on Hybrid Automata and Composite Lyapunov Function. *IEEE Transactions on Intelligent Transportation Systems*. doi: 10.1109/TITS.2009.2026451.
- Netto, M.S., Chaib, S., and Mammar, S. (2004). Lateral adaptive control for vehicle lane keeping. *In Proceedings Of The American Control Conference*. Boston, MA.
- Peng, H. and Tomizuka, M. (1993). Preview Control for Vehicle Lateral Guidance in Highway Automation. *Journal of Dynamic Systems, Measurement, and Control*, 115, 679–687.
- Pomerleau, D.A. (1995). RALPH: Rapidly Adapting Lateral Position Handler. *In Proc. IEEE Intelligent Vehicle Symposium*.
- Rajamani, R. (2006). *Vehicle Dynamics and Control*. Springer.
- Roland, R.D. and Sheridan, T.B. (1967). Simulation study of the driver’s control of sudden changes in previewed path. Technical report, MIT, Department of Mechanical Engineering.
- Rossetter, E.J. and Gerdes, J.C. (2002). A Study of Lateral Vehicle Control Under a Virtual Force Framework. *In Proc. International Symposium on Advanced Vehicle Control*.
- Shin, D., Sim, S., Ryu, J., Lee, J., and Lee, I. (2008). Vision Based Path-Following Control System Using Back-stepping Control Methodology. *SAE*, Paper 2008-01-0202.
- Svedenius, J. (2007). *Tire Modeling and Friction Estimation*. Ph.D. thesis, Department of Automatic Control, Lund University, Lund, Sweden.